Competitive adsorption of ofloxacin enantiomers to goethite : experiments and modelling

Environmental Chemistry

Qin, Xiaopeng; Zhong, Xiaofei; Du, Ping; Chen, Juan; Jia, Junfeng et al

Research Paper

Competitive adsorption of ofloxacin enantiomers to goethite: experiments and modelling

Xiaopeng Qin, [ID] [A,B,E] *Xiaofei Zhong,* [B,C] *Ping Du,* [A,B] *Juan Chen,* [A,B]
Junfeng Jia, [A,B] *Ying He,* [A,B] *Fei Liu* [C,E] *and Liping Weng* [D]

[A]Department of Technology Assessment, Technical Centre for Soil, Agricultural and Rural Ecology
and Environment, Ministry of Ecology and Environment, Beijing 100012, China.
[B]State Key Laboratory of Environmental Criteria and Risk Assessment, Institute of Soil and Solid,
Chinese Research Academy of Environmental Sciences, Beijing 100012, China.
[C]Key Laboratory of Groundwater Circulation and Environmental Evolution, Ministry of Education,
School of Water Resources and Environment, China University of Geosciences (Beijing),
Beijing 100083, China.
[D]Department of Soil Quality, Wageningen University PO Box 47, 6700 AA, Wageningen,
The Netherlands.
[E]Corresponding authors. Email: qinxp@craes.org.cn; feiliu@cugb.edu.cn

Environmental context. The concentration, types and distribution of antibiotics in soils can have environmental effects and can be modelled using laboratory systems. Adsorption of ofloxacin (OFL) and levofloxacin (LEV) enantiomers to goethite can probe this behaviour and each binds differently to the solid phase. The different behaviour of LEV and OFL in relation to solid-solution partitioning will affect their environmental fate.

Abstract. The adsorption of ofloxacin enantiomers, namely levofloxacin (LEV) and ofloxacin (OFL), to goethite was investigated using batch experiments. Structural information of aqueous and adsorbed LEV or OFL was obtained with ultraviolet–visible (UV-Vis), three-dimensional excitation–emission matrix (EEM) and attenuated total reflectance Fourier-transform infrared (ATR-FTIR) spectroscopic methods. The results indicated that LEV molecules formed a bridging bidentate complex ($\equiv(FeO)_2$–LEV) with the surface of goethite, and OFL formed a monodentate complex ($\equiv FeO$–OFL). The adsorption of OFL to goethite was stronger than that of LEV, owing to differences in their physicochemical properties and bonding modes. The adsorption of LEV and OFL to goethite in single systems was well simulated using the charge distribution multi-site complexation (CD-MUSIC) model, but their adsorption in the LEV–OFL–goethite systems was overestimated at pH ~5.2 and high concentrations of LEV–OFL mixture (19.59 μM), in which the predicted amounts of adsorbed LEV and OFL were higher (20.0, 30.8 %) than the experimental results. Compared with the unprotonated LEV or OFL, the protonated (>99.9 %) ones were mainly adsorbed to the surface of goethite, and the single species may be used during their following modelling.

Introduction

Pharmaceuticals frequently used in human and veterinary treatments are often detected in soils, sediments and waters, and have an adverse influence on the microbial communities in the environment (Córdova-Kreylos and Scow 2007; Zhou et al. 2020). As reported by Sanganyado et al. (2017), at least 50 % of pharmaceuticals in current use are chiral compounds. The differences in the structures of chiral pharmaceuticals may alter their environmental fate and influence on microorganisms (Liu et al. 2005; Maia et al. 2018; Buerge et al. 2019).

Adsorption is a key process controlling the transport and degradation of chiral pharmaceuticals and other organic compounds in the environment. As reported previously, the adsorption of (L)-enantiomers (e.g. tryptophan, phenylalanine, tyrosine) to coated magnetic nanoparticles was stronger than of the corresponding (D)-enantiomers (Ghosh et al. 2011). Additionally, the adsorption coefficient (K_d) values of the (S)-enantiomers of acebutolol and metoprolol to sludge were approximately twice those of the (R)-enantiomers, but there were no significant differences in K_d values of the enantiomers of pindolol and propranolol (Sanganyado et al. 2016). The K_d values of (R)- and (S)-enantiomers of metalaxyl (Celis et al. 2015) and abscisic acid (Gámiz et al. 2016) to soils from initial racemic solutions were similar. The adsorption of (R)- and (S)-enantiomers of mecoprop (or dichlorprop) to soils were in the same ratio (Matallo et al. 1998). Consequently, the adsorption behaviours of various chiral organic compounds to the same adsorbent are quite different.

Levofloxacin (LEV) and ofloxacin (OFL) are widely used chiral antibiotics, and LEV has a higher antibacterial activity. In almost all field studies, LEV and OFL in soils and waters cannot

be separated and analysed by high performance liquid chromatography (HPLC) (Golet et al. 2001; Chen et al. 2018), and thus LEV is usually mistaken for OFL, which leads to assessing their adsorption processes and influence on microorganisms inaccurately. The adsorption behaviours of LEV and OFL to the same mineral or soil have seldom been reported. The Langmuir constant (K) of LEV was 1.25 times larger than that of OFL for their adsorption to aluminium hydroxide, but their maximum adsorption capacities were similar (Tanaka et al. 1993). As a result, it can be seen that the adsorption of chiral pharmaceuticals to minerals is still not well understood.

In the present work, LEV and OFL were chosen as an example of chiral pharmaceuticals. Goethite (α-FeOOH), a common iron hydroxide in soils and sediments, was used as the model adsorbent. First, the Charge Distribution Multi-Site Complexation (CD-MUSIC) model (Hiemstra et al. 1989; Hiemstra and Van Riemsdijk 1996), which has previously been used to predict the adsorption of LEV (Qin et al. 2014b) or OFL (Paul et al. 2014) to goethite, was used to describe the adsorption of chiral pharmaceuticals (i.e. LEV, OFL) to goethite in single systems. Second, the model with the same parameters derived from the single adsorption studies was used to predict the competitive adsorption of LEV and OFL in LEV–OFL–goethite systems. This is the first modelling exercise to describe the competitive adsorption of chiral pharmaceuticals on minerals.

Experimental

Materials

Goethite was synthesised by the hydrolysing and aging method (Hiemstra et al. 1989; Antelo et al. 2005). It was proved to be pure α-FeOOH according to the X-ray diffraction (XRD) (Rigaku, D/MAX 2500PC) result. The specific surface area of goethite is 99.0 ± 0.4 m^2 g^{-1} determined with the Brunauer–Emmett–Teller (BET) method. The pristine point of zero charge (PZC) of goethite synthesised using the same method is between 9.0 and 9.3 (Antelo et al. 2005; Weng et al. 2008).

Levofloxacin (LEV) and ofloxacin (OFL) ($>98.0\%$) were obtained from Tokyo Chemical Industry Co. In our study, the OFL contained 52% LEV, and this is named LEV–OFL mixture in the following sections. Another ofloxacin (OFL) ($>99.0\%$) standard was obtained from United States Pharmacopeia (USP), and no LEV was found in it. Owing to the limited amount (100 mg) of OFL standard, the concentration of OFL in some experiments is lower than that of LEV. Both LEV and OFL molecules contain a carboxyl group and a piperazinyl group. The protonation constants (pK_{a1} and pK_{a2}) of LEV are 6.02 and 8.15 (Sousa et al. 2012), and the values for OFL are 6.05 and 8.22 (Ross and Riley 1990). Methanol (HPLC grade) was obtained from JT Baker. Other chemicals used in this study were analytical reagent grade or higher. MilliQ water was used in all experiments.

UV-visible, excitation–emission matrix and attenuated total reflectance Fourier-transform infrared spectroscopy

Structural information on aqueous LEV and OFL was obtained using ultraviolet-visible (UV-vis) and three-dimensional excitation–emission matrix (EEM) spectroscopic methods. UV-Vis spectra of LEV (5, 10, 20 μM), OFL (5, 10, 20 μM) and LEV–OFL mixture (10, 20, 40 μM) were measured from 200 to 540 nm at 1-nm resolution with a UV-vis spectrophotometer (Hitachi U-3010). The EEM spectra of LEV (0.1, 0.2 μM), OFL (0.1, 0.2 μM) and LEV–OFL mixture (0.2, 0.4 μM) were

measured with a fluorescence spectrophotometer (Hitachi F-7000). The emission and excitation wavelengths were in the range of 250–600 and 200–500 nm respectively.

Solid samples for attenuated total reflectance Fourier-transform infrared (ATR-FTIR) analysis were obtained following the same procedure used in adsorption studies but at higher concentrations of the antibiotics (5 mM LEV, 2.5 mM OFL and 10 mM LEV–OFL mixture). Goethite samples were prepared using the method reported by Kubicki et al. (2012) and modified in this study. After equilibrium, samples were centrifuged at 35190 g to separate the solids, and dried at 45°C for 48 h (Zhao et al. 2017). Aqueous samples (0.25 mM LEV, 0.5 mM OFL and 1 mM LEV–OFL mixture) were also prepared at pH 5. The FTIR spectra of solid and aqueous samples were recorded with an ATR-FTIR spectrometer (Nicolet iS10). Spectra were obtained by averaging 32 scans at 4 cm^{-1} resolution.

Single adsorption studies

Adsorption edges of LEV or OFL were obtained by batch experiments. Polyethylene centrifuge tubes (50 mL) were used, and were flushed with ultrapure N$_2$ to minimise the influence of CO$_2$ in the air. Varying concentrations of LEV or OFL solution (10 mL) and goethite suspension (10 mL of 2.0 g L^{-1}) (or MilliQ water as the control samples) were added into the tubes. NaCl (0.01 M) was used as the background solution. The final total concentrations of LEV (or OFL) were 3, 5 and 10 μM (1, 3, 5, 7.5 and 10 μM). After mixing, the concentration of goethite was 1.0 g L^{-1}. Solution pH was adjusted in the range of 3–10 using acid (0.01 M HCl) or base (0.01 M NaOH).

The effect of initial concentrations of LEV or OFL on adsorption was studied using adsorption envelopes. The suspensions were prepared in a similar procedure to that mentioned above. The initial concentrations of LEV or OFL were in the range of 1–10 μM. The final solution pH was 5.0.

The antibiotic–goethite suspensions were shaken at 175 rpm and 25°C for 24 h in the dark. Final pH values of all the samples were analysed after equilibrium. The samples were centrifuged at 35190 g for 20 min, and the supernatant was stored at 4°C in the refrigerator for later measurements. All adsorption experiments were carried out in triplicate.

Binary adsorption studies

Competitive adsorption studies of LEV and OFL to goethite were carried out following a similar method. The amount of goethite was 1.0 g L^{-1}. During the adsorption edges studies, the final concentrations of LEV–OFL mixture were 5, 10 and 20 μM. In adsorption isotherm studies, the initial concentrations of LEV–OFL mixture were in the range of 4–20 μM, and the final solution pH was 5.0.

Chemical analysis

In single adsorption experiments, the concentration of LEV or OFL in solutions was measured using HPLC (Qin et al. 2014a).

In binary adsorption experiments, the concentrations of LEV and OFL were simultaneously analysed using the method reported by Shao et al. (2008), and modified in the present study. A Shimadzu LC-20AT HPLC system with an Agilent C18 column (4.6 × 250 mm, 5 μm particle size) coupled to a diode array detector (DAD; Shimadzu SPD-M20A) was used. LEV and OFL were detected at 293 nm. The mobile phase used consisted of 20% methanol and 80% water (4 mM L-isoleucine and 3 mM CuSO$_4$). The elution rate was 1.0 mL min^{-1}. The injection volume was 20 μL. The column temperature was 40°C.
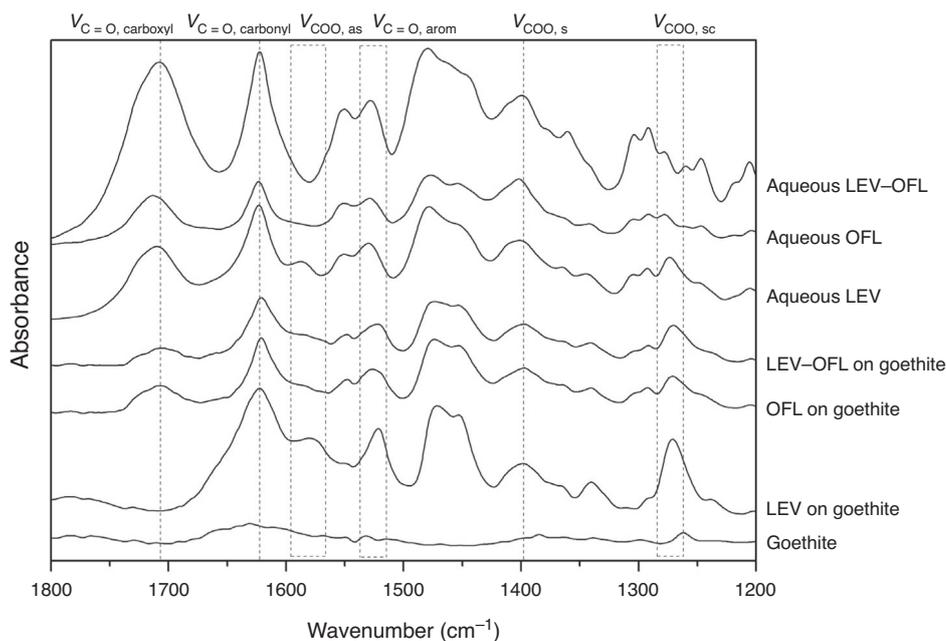
Fig. 1. ATR-FTIR spectra of OFL, LEV, and OFL–LEV mixture before and after adsorption to goethite at pH 5.

The amounts of OFL or LEV adsorbed on goethite were calculated according to differences in the initial and equilibrium concentrations in the solution. According to the results of control samples (without goethite), there were no significant losses in the concentration of LEV or OFL.

Modelling approach

The adsorption data for LEV and OFL were simulated using the CD-MUSIC model (Hiemstra et al. 1989; Hiemstra and Van Riemsdijk 1996), which was similar to the modelling of LEV adsorption to goethite (Qin et al. 2014b). The CD values of LEV were from a previous study (Qin et al. 2018), and were also considered in the calculation for OFL owing to their very similar structures and bonding modes. The adsorption affinity constants (log K) of LEV and OFL to goethite were derived by fitting. During the modelling process, 40 or 24 adsorption data points (each one being the average value of three samples) of OFL and LEV at all initial concentrations (1–10 µM) were fitted simultaneously. The log K values for LEV–goethite or OFL–goethite complexes were calculated on the basis of the root mean square error (RMSE).

Model calculations were performed using the *ECOSAT 4.9* program (Keizer and Van Riemsdijk 1998). Optimisation of the parameters by assessing the differences between modelling results and experimental data was carried out with *Microsoft Excel 2007* software.

Results and discussion

The structures of adsorbed LEV and OFL

The UV-vis spectra of aqueous OFL, LEV and LEV–OFL mixture are shown in Fig. S1 (Supplementary material). The spectra of aqueous OFL, LEV and OFL–LEV mixture are similar, and two peaks are observed at ~301 and 328 nm. At the same concentrations, the UV absorbance of OFL is much stronger than that of LEV. Based on the data depicted in Fig. S1, the calculated molar absorptivity values (at 301 nm) of LEV and OFL are 1.92×10^4 and 2.13×10^4 mol L^{-1} cm^{-1} respectively. The molar absorptivity

(at 301 nm) of LEV–OFL mixture is 1.71×10^4 mol L^{-1} cm^{-1}, which is smaller than the value for LEV and OFL. In all the EEM spectra of OFL, LEV and LEV–OFL mixture, there is a peak around $\lambda_{em}/\lambda_{ex}$ of 500/290 nm (Fig. S2, Supplementary material). The fluorescence intensity of LEV is larger than that of OFL, which is the opposite of their UV absorbance (Fig. S1). Different fluorescence or UV intensity values of LEV and OFL have also been found during their measurement with HPLC coupled to a fluorescence (Zeng et al. 1999) or UV/DAD detector (Yan and Row 2007; present study). Consequently, according to the UV-vis and EEM results, the structures of LEV and OFL in solutions are different, which may eventually affect their complexation with the same cations (e.g. Ca^{2+}, Mg^{2+}, Fe^{3+}) (Urbaniak and Kokot 2009) and adsorption to the same mineral (Tanaka et al. 1993). In order to investigate the interactions between LEV, OFL and goethite, ATR-FTIR measurements were also conducted.

Fig. 1 shows the ATR-FTIR spectra of OFL, LEV and LEV–OFL mixture before and after adsorption to goethite. LEV or OFL has strong absorbance bands such as those at 1708 cm^{-1} ($v_{C=O}$, carboxyl), 1621 cm^{-1} ($v_{C=O}$, carbonyl), 1582 cm^{-1} ($v_{COO,as}$), 1526 cm^{-1} ($v_{C=C}$, arom), 1398 cm^{-1} ($v_{COO,s}$), and 1271 cm^{-1} (v_{COOH}/δ_{C-OH}), which are consistent with the reported results for LEV (Le-Deygen et al. 2017; Yan and Niu 2017), OFL (Goyne et al. 2005; Paul et al. 2014; Zhao et al. 2019) and ciprofloxacin (Trivedi and Vasudevan 2007).

We note that there were nevertheless some differences in the spectra of LEV and OFL (Fig. 1): (1) The carboxyl absorbance band ($v_{C=O}$, ~1710 cm^{-1}) of LEV disappeared after adsorption to goethite, indicating the carboxyl groups were involved during the reaction, which was not observed in the other spectra (i.e. OFL), so carboxyl ($v_{C=O}$) was not involved in the adsorption of OFL to goethite; (2) spectral red shifts were only observed in the asymmetric stretching mode of the deprotonated carboxylate groups ($v_{COO,as}$, ~1587 cm^{-1}) of LEV during its adsorption to goethite; (3) spectral red shifts were observed in the scissoring of the deprotonated carboxylate groups ($v_{COO,sc}$, ~1276 cm^{-1}) of OFL (or LEV–OFL mixture, not LEV) during its adsorption to goethite.

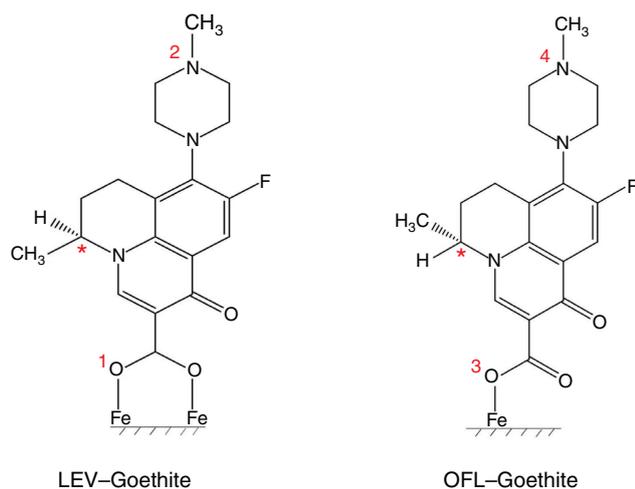**Fig. 2.** The structures for LEV and OFL complexation with the surface of goethite.

Fig. 3. Adsorption of single LEV (a), and OFL (b) to goethite under different pH conditions in 0.01 M NaCl. Error bars ($\pm$1 s.d., $n = 3$) are shown in figures. Solid (LEV) and dashed (OFL) lines in figures are model calculations using the parameters listed in Table 1.

Spectral red shifts were observed in the aromatic groups (v_{Ar}, $\sim$1526 cm^{-1}) of the antibiotics during their adsorption to goethite, which could be attributed to the complexation between LEV or OFL molecules and Fe ions on the surface of goethite. A similar spectral red shift phenomenon was also observed in UV-vis measurements for OFL adsorption to TiO$_2$ (Paul et al. 2012). No significant changes were found in the carbonyl absorbance bands ($v_{C=O}$, 1621 cm^{-1}), and symmetric stretching mode of the deprotonated carboxylate groups ($v_{COO,s}$, $\sim$1380 cm^{-1}), so these functional groups were not involved in the adsorption processes.

As reported previously (Tackett 1989; Trivedi and Vasudevan 2007), the difference (Δv) between the asymmetric and symmetric carboxylic stretch ($\Delta v = v_{COO,as} - v_{COO,s}$) was used to identify the bonding mode of carboxyl groups (–COOH) with metals or minerals (e.g. goethite), in which $\Delta v_{goethite-COO}$ is the difference between $v_{COO,as}$ and $v_{COO,s}$ of LEV or OFL adsorbed to goethite, and $\Delta v_{free\ COO}$ is the difference between $v_{COO,as}$ and $v_{COO,s}$ of LEV or OFL in solutions (control samples, without goethite). A Δv of the mineral–carboxylate complexes ($\Delta v_{goethite-COO}$) greater than the Δv of the free carboxylate complexes ($\Delta v_{Free\ COO}$) indicates a monodentate complex, a $\Delta v_{goethite-COO} < \Delta v_{Free\ COO}$ a bidentate chelate, and a $\Delta v_{goethite-COO} \approx \Delta v_{Free\ COO}$ a bridging bidentate complex. In this study, the calculated $\Delta v_{goethite-COO}$ and $\Delta v_{Free\ COO}$ values of LEV were 183 and 186 cm^{-1}, so LEV formed a bridging bidentate complex with goethite (Fig. 2).

It was difficult to identify the bonding mode of OFL and goethite using the same method, because the absorbance band ($v_{COO,as}$, $\sim$1582 cm^{-1}) of OFL was not observed in this study. As discussed above, (1) the carboxyl group ($v_{C=O}$) was not involved during the adsorption of OFL to goethite; and (2) spectral red shifts were observed in $v_{COO\ sc}$ of OFL adsorbed to goethite, which was involved in the adsorption process. Consequently, monodentate is the most likely complex during the adsorption of OFL to goethite (Fig. 2).

Modelling LEV or OFL adsorption in the single system

In the single system, adsorption of LEV or OFL to goethite is shown in Fig. 3. In a previous paper (Qin et al. 2014b), LEV adsorption to goethite has been discussed. The curve for the adsorption of OFL to goethite is also bell-shaped (Fig. 3b). The maximum amounts of adsorbed OFL are reached at pH
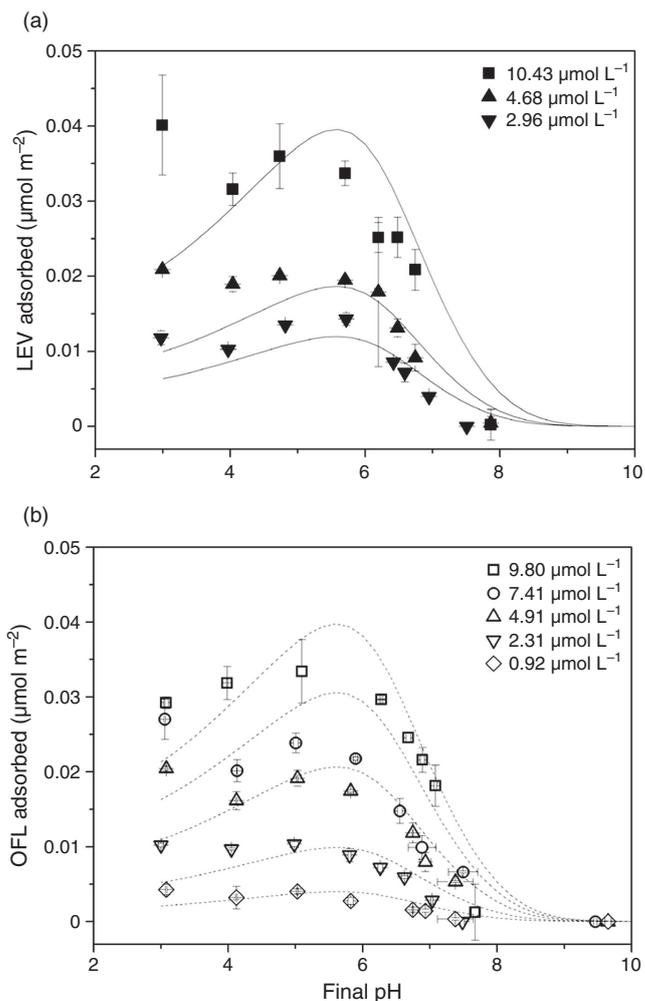
$\sim$5.5, and decrease beyond this pH range, similarly to those of LEV (Qin et al. 2014b) and OFL (Paul et al. 2014).

In the present study, bridging bidentate and monodentate species were respectively formed during the adsorption of LEV and OFL to goethite (Fig. 2). As shown in Fig. 3, LEV or OFL adsorption to goethite is well described by the CD-MUSIC model (RMSE $<$0.006, $n = 24$ or 40), using the parameters listed in Table 1. When the initial concentration of LEV or OFL is 10 µM, the calculated maximum amounts of LEV and OFL are 0.038 and 0.040 µmol m^{-2} respectively. OFL adsorption to goethite is a bit stronger than that of LEV (Fig. S3, Supplementary material); the same results are also observed in the adsorption isotherm studies at high concentrations of antibiotics ($>$5 µM) (Fig. S4, Supplementary material), which is because their physicochemical properties (e.g. pK_a) and bonding modes on goethite surface are different.

In the next section, we use the CD-MUSIC model with the same parameters to predict their competitive adsorption in the LEV–OFL–goethite systems.

Adsorption of LEV and OFL in binary system

The competitive adsorption of LEV–OFL mixture to goethite is shown in Fig. 4. At pH $\sim$5, the amounts of adsorbed LEV and

Table 1.   Surface species and CD-MUSIC model parameters of goethite, LEV–goethite complexes and OFL–goethite complexes

Site density, capacitance and other basic properties of goethite are from Hiemstra et al. (2010). Δz_0, Δz_1 and Δz_2 are charge attributed to the 0-plane, 1-plane and 2-plane. Log K values for LEV–goethite and OFL–goethite complexes were calculated on the basis of the root mean square error (RMSE); $RMSE_{LEV} =$ 0.00584 ($n = 24$), $RMSE_{OFL} = 0.00268$ ($n = 40$). LEV and OFL are the zwitterionic or neutral species of LEV and OFL. C_1 and C_2 are inner and outer layer capacitances, respectively

Basic parameters	PZC	Site density (nm^{-2})		Capacitance (F m^{-2})	
		$-Fe_1OH^{-0.5}$	$-Fe_3O^{-0.5}$	C_1	C_2
	9.0	3.45	2.70	0.93	0.75

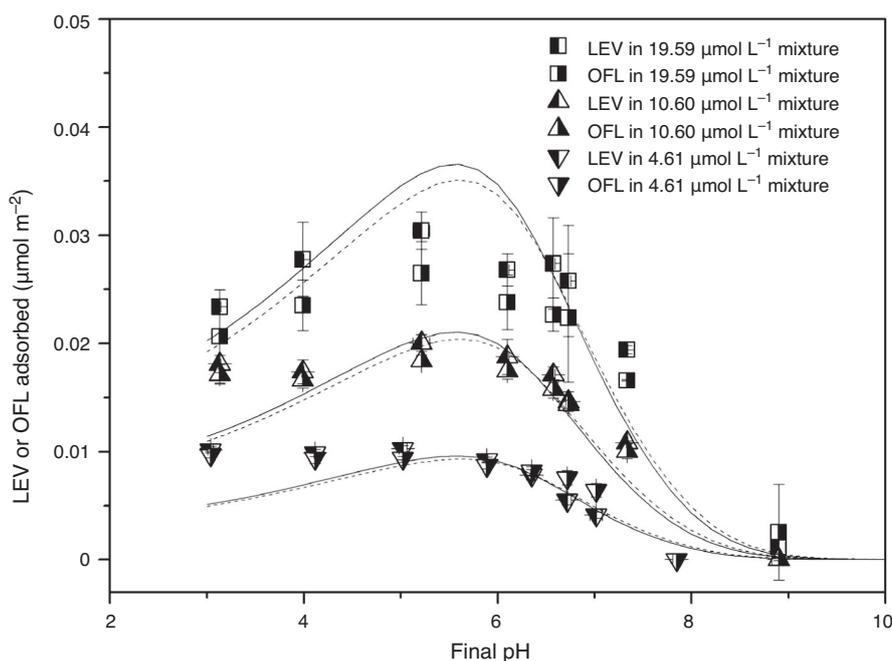|	Sites		Charge distribution			Ions or ligands				log K
Surface species	$-Fe_1OH^{-0.5}$	$-Fe_3O^{-0.5}$	Δz_0	Δz_1	Δz_2	H$^+$	Na$^+$	Cl$^-$	LEV or OFL	
$\equiv FeOH_2^{+0.5}$	1	0	1	0	0	1	0	0	0	9.00
$\equiv Fe_3OH^{+0.5}$	0	1	1	0	0	1	0	0	0	9.00
$\equiv FeOH\cdots Na^{+0.5}$	1	0	0	1	0	0	1	0	0	-0.60
$\equiv Fe_3O\cdots Na^{+0.5}$	0	1	0	1	0	0	1	0	0	-0.60
$\equiv FeOH_2\cdots Cl^{-0.5}$	1	0	1	-1	0	1	0	1	0	8.55
$\equiv FeOH\cdots Cl^{-0.5}$	1	0	1	-1	0	1	0	1	0	8.55
$\equiv (FeO)_2HLEV^{+1}$	2	0	1.1	-0.1	1	2	0	0	1	22.46
$\equiv (FeO)_2LEV^0$	2	0	1.1	-0.1	0	1	0	0	1	6.00
$\equiv FeOHOFL^{+0.5}$	1	0	0.1	-0.1	1	1	0	0	1	13.28
$\equiv FeOOFL^{-0.5}$	1	0	0.1	-0.1	0	0	0	0	1	0.55

Fig. 4.   Adsorption of LEV or OFL in LEV–OFL mixture under different pH conditions in 0.01 M NaCl. Error bars (± 1 s.d., $n = 3$) are shown in figures. Solid (LEV) and dashed (OFL) lines in figures are model calculations using the parameters listed in Table 1.

OFL are respectively 0.030 and 0.026 μmol m^{-2} in 20 μM mixture, which is smaller than their corresponding values (0.036 and 0.033 μmol m^{-2}) in single systems (Fig. 3). Similar competition between LEV and OFL in binary studies is also found in the adsorption isotherm studies (Fig. S4). As a consequence, in the LEV–OFL–goethite systems, LEV and OFL compete for the sites on the goethite surface during the adsorption process.

The adsorption data of LEV and OFL in binary systems were simulated using the CD-MUSIC model with the same parameters (Table 1) derived from the single adsorption studies. The fit is good (Fig. 4), except for the simulation at pH ~5.2 and high concentration of LEV–OFL mixture (19.59 μM), in which the predicted amounts of adsorbed LEV–OFL are higher (20.0, 30.8 %) than the experimental results.

In LEV–OFL mixture, there are small differences in the initial concentrations of LEV and OFL (52 : 48 % w/w), which also affect the adsorption amounts of LEV and OFL to goethite during the experiments. In order to compare the adsorption between LEV and OFL more exactly, their adsorption processes were calculated using the CD-MUSIC model (Fig. S5, Supplementary material). Compared with LEV, more OFL was adsorbed to goethite (pH < 6), especially in the pH range of 5–7, but there were no significant differences at pH > 9. This was because OFL has a larger protonation constant (pK_{a1}) than LEV. Compared with the unprotonated LEV or OFL, the protonated (>99.9 %) ones were mainly adsorbed to the surface of goethite, and the single species may be used during their following modelling.

Conclusions

The adsorption behaviours of LEV and OFL to goethite were quite different. The ATR-FTIR spectroscopic evidence indicated that LEV formed a bridging bidentate complex with the goethite surface, and OFL formed a monodentate complex. OFL adsorption to goethite is stronger than that of LEV. The adsorption of LEV and OFL to goethite was well simulated by the CD-MUSIC model. In the natural environment, compared with OFL (or LEV–OFL mixture), more free LEV may exist in soils and sediments, and be released into groundwater, which would increase its toxicity to microorganisms.

Supplementary material

The UV-Vis spectra, EEM spectra, adsorption isotherm of LEV and OFL, and the calculated amounts of LEV and OFL adsorbed to goethite in single or binary systems are available on the Journal's website.

Conflicts of interest

The authors declare no conflicts of interest.

Acknowledgements

References

Antelo J, Avena M, Fiol S, López R, Arce F (2005). Effects of pH and ionic strength on the adsorption of phosphate and arsenate at the goethite–water interface. *Journal of Colloid and Interface Science* **285**, 476–486. doi:10.1016/J.JCIS.2004.12.032

Buerge IJ, Bächli A, Kasteel R, Portmann R, López-Cabeza R, Schwab LF, Poiger T (2019). Behavior of the chiral herbicide imazamox in soils: pH-dependent, enantioselective degradation, formation and degradation of several chiral metabolites. *Environmental Science & Technology* **53**, 5725–5732. doi:10.1021/ACS.EST.8B07209

Celis R, Gámiz B, Facenda G, Hermosín MC (2015). Enantioselective sorption of the chiral fungicide metalaxyl on soil from non-racemic aqueous solutions: environmental implications. *Journal of Hazardous Materials* **300**, 581–589. doi:10.1016/J.JHAZMAT.2015.07.059

Chen L, Lang H, Liu F, Jin S, Yan T (2018). Presence of antibiotics in shallow groundwater in the northern and south-western regions of China. *Ground Water* **56**, 451–457. doi:10.1111/GWAT.12596

Córdova-Kreylos AL, Scow KM (2007). Effects of ciprofloxacin on salt marsh sediment microbial communities. *The ISME Journal* **1**, 585–595. doi:10.1038/ISMEJ.2007.71

Gámiz B, Hermosín MC, Celis R (2016). Sorption, persistence and leaching of abscisic acid in agricultural soils: an enantiomer-selective study. *Geoderma* **269**, 112–118. doi:10.1016/J.GEODERMA.2016.01.024

Ghosh S, Badruddoza AZM, Uddin MS, Hidajat K (2011). Adsorption of chiral aromatic amino acids onto carboxymethyl-*b*-cyclodextrin bonded Fe₃O₄/SiO₂ core–shell nanoparticles. *Journal of Colloid and Interface Science* **354**, 483–492. doi:10.1016/J.JCIS.2010.11.060

Golet EM, Alder AC, Hartmann A, Ternes TA, Giger W (2001). Trace determination of fluoroquinolone antibacterial agents in urban wastewater by solid-phase extraction and liquid chromatography with fluorescence detection. *Analytical Chemistry* **73**, 3632–3638. doi:10.1021/AC0015265

Goyne KW, Chorover J, Kubicki JD, Zimmerman AR, Brantley SL (2005). Sorption of the antibiotic ofloxacin to mesoporous and non-porous alumina and silica. *Journal of Colloid and Interface Science* **283**, 160–170. doi:10.1016/J.JCIS.2004.08.150

Hiemstra T, Van Riemsdijk WH (1996). A surface structural approach to ion adsorption: the charge distribution (CD) model. *Journal of Colloid and Interface Science* **179**, 488–508. doi:10.1006/JCIS.1996.0242

Hiemstra T, De Wit JCM, Van Riemsdijk WH (1989). Multisite proton adsorption modeling at the solid/solution interface of (hydr)oxides: a new approach: II. Application to various important (hydr)oxides. *Journal of Colloid and Interface Science* **133**, 105–117. doi:10.1016/0021-9797(89)90285-3

Hiemstra T, Antelo J, Rahnemaie R, Van Riemsdijk WH (2010). Nanoparticles in natural systems I: The effective surface area of the natural oxide fraction in field samples. *Geochimica et Cosmochimica Acta* **74**, 41–58. doi:10.1016/J.GCA.2009.10.018

Keizer MG, Van Riemsdijk WH (1998). ECOSAT: equilibrium calculation of speciation and transport. Technical report of the Soil Quality Department. (Wageningen University: Wageningen).

Kubicki JD, Paul KW, Kabalan L, Zhu Q, Mrozik MK, Aryanpour M, Pierre-Louis AM, Strongin DR (2012). ATR-FTIR and density functional theory study of the structures, energetics, and vibrational spectra of phosphate adsorbed onto goethite. *Langmuir* **28**, 14573–14587. doi:10.1021/LA303111A

Le-Deygen IM, Skuredina AA, Uporov IV, Kudryashova EV (2017). Thermodynamics and molecular insight in guest–host complexes of fluoroquinolones with β-cyclodextrin derivatives, as revealed by ATR-FTIR spectroscopy and molecular modeling experiments. *Analytical and Bioanalytical Chemistry* **409**, 6451–6462. doi:10.1007/S00216-017-0590-5

Liu W, Gan J, Schlenk D, Jury WA (2005). Enantioselectivity in environmental safety of current chiral insecticides. *Proceedings of the National Academy of Sciences of the United States of America* **102**, 701–706. doi:10.1073/PNAS.0408847102

Maia AS, Tiritan ME, Castro P (2018). Enantioselective degradation of ofloxacin and levofloxacin by the bacterial strains *Labrys portucalensis* F11 and *Rhodococcus* sp. FP1. *Ecotoxicology and Environmental Safety* **155**, 144–151. doi:10.1016/J.ECOENV.2018.02.067

Matallo M, Romero E, Sánchez-Rasero F, Peña A, Dios G (1998). Adsorption of mecoprop and dichlorprop on calcareous and organic matter-amended soils: comparative adsorption of racemic and pure enantiomeric forms. *Journal of Environmental Science and Health. Part B, Pesticides, Food Contaminants, and Agricultural Wastes* **33**, 51–66. doi:10.1080/03601239809373129

Paul T, Machesky ML, Strathmann TJ (2012). Surface complexation of the zwitterionic fluoroquinolone antibiotic ofloxacin to nano-anatase TiO₂ photocatalyst surfaces. *Environmental Science & Technology* **46**, 11896–11904. doi:10.1021/ES302097K

Paul T, Liu J, Machesky ML, Strathmann TJ (2014). Adsorption of zwitterionic fluoroquinolone antibacterials to goethite: a charge distribution-multisite complexation model. *Journal of Colloid and Interface Science* **428**, 63–72. doi:10.1016/J.JCIS.2014.04.034

Qin X, Liu F, Wang G, Weng L, Li L (2014a). Adsorption of levofloxacin onto goethite: effects of pH, calcium and phosphate. *Colloids and Surfaces. B, Biointerfaces* **116**, 591–596. doi:10.1016/J.COLSURFB.2013.09.056

Qin X, Liu F, Wang G, Li L, Wang Y, Weng L (2014b). Modeling of levofloxacin adsorption to goethite and the competition with phosphate. *Chemosphere* **111**, 283–290. doi:10.1016/J.CHEMOSPHERE.2014.04.032

Qin X, Du P, Chen J, Liu F, Wang G, Weng L (2018). Effects of natural organic matter with different properties on levofloxacin adsorption to

goethite: experiments and modeling. *Chemical Engineering Journal* **345**, 425–431. doi:10.1016/J.CEJ.2018.03.125

Ross DL, Riley CM (1990). Aqueous solubilities of some variously substituted quinolone antimicrobials. *International Journal of Pharmaceutics* **63**, 237–250. doi:10.1016/0378-5173(90)90130-V

Sanganyado E, Fu Q, Gan J (2016). Enantiomeric selectivity in adsorption of chiral β-blockers on sludge. *Environmental Pollution* **214**, 787–794. doi:10.1016/J.ENVPOL.2016.04.091

Sanganyado E, Lu Z, Fu Q, Schlenk D, Gan J (2017). Chiral pharmaceuticals: a review on their environmental occurrence and fate processes. *Water Research* **124**, 527–542. doi:10.1016/J.WATRES.2017.08.003

Shao B, Sun X, Zhang J, Hu J, Dong H, Yang Y (2008). Determination of ofloxacin enantiomers in sewage using two-step solid-phase extraction and liquid chromatography with fluorescence detection. *Journal of Chromatography. A* **1182**, 77–84. doi:10.1016/J.CHROMA.2007.12.073

Sousa I, Claro V, Pereira JL, Amaral A, Cunha-Silva L, Castro B, Feio M, Pereira E, Gameiro P (2012). Synthesis, characterization and antibacterial studies of a copper(II) levofloxacin ternary complex. *Journal of Inorganic Biochemistry* **110**, 64–71. doi:10.1016/J.JINORGBIO.2012.02.003

Tackett JE (1989). FT-IR characterization of metal acetates in aqueous solution. *Applied Spectroscopy* **43**, 483–489. doi:10.1366/0003702894202931

Tanaka M, Kurata T, Fujisawa C, Ohshima Y, Aoki H, Okazaki O, Hakusui H (1993). Mechanistic study of inhibition of levofloxacin absorption by aluminum hydroxide. *Antimicrobial Agents and Chemotherapy* **37**, 2173–2178. doi:10.1128/AAC.37.10.2173

Trivedi P, Vasudevan D (2007). Spectroscopic investigation of ciprofloxacin speciation at the goethite–water interface. *Environmental Science & Technology* **41**, 3153–3158. doi:10.1021/ES061921Y

Urbaniak B, Kokot ZJ (2009). Analysis of the factors that significantly influence the stability of fluoroquinolone–metal complexes. *Analytica Chimica Acta* **647**, 54–59. doi:10.1016/J.ACA.2009.05.039

Weng L, Van Riemsdijk WH, Hiemstra T (2008). Humic nanoparticles at the oxide–water interface: interactions with phosphate ion adsorption. *Environmental Science & Technology* **42**, 8747–8752. doi:10.1021/ES801631D

Yan B, Niu CH (2017). Modeling and site energy distribution analysis of levofloxacin sorption by biosorbents. *Chemical Engineering Journal* **307**, 631–642. doi:10.1016/J.CEJ.2016.08.065

Yan H, Row KH (2007). Rapid chiral separation and impurity determination of levofloxacin by ligand-exchange chromatography. *Analytica Chimica Acta* **584**, 160–165. doi:10.1016/J.ACA.2006.11.023

Zeng S, Zhong J, Hu J, Pan L, Li Y (1999). High-performance liquid chromatography separation and quantitation of ofloxacin enantiomers in rat microsomes. *Journal of Chromatography. B, Biomedical Sciences and Applications* **728**, 151–155. doi:10.1016/S0378-4347(99)00085-7

Zhao Y, Liu F, Qin X (2017). Adsorption of diclofenac onto goethite: adsorption kinetics and effects of pH. *Chemosphere* **180**, 373–378. doi:10.1016/J.CHEMOSPHERE.2017.04.007

Zhao X, Hu Z, Yang X, Cai X, Wang Z, Xie X (2019). Non-covalent interactions between fluoroquinolone antibiotics with dissolved organic matter: a ^{1}H NMR binding site study and multispectroscopic methods. *Environmental Pollution* **248**, 815–822. doi:10.1016/J.ENVPOL.2019.02.077

Zhou Z, Zhang Z, Feng L, Zhang J, Li Y, Lu T, Qian H (2020). Adverse effects of levofloxacin and oxytetracycline on aquatic microbial communities. *The Science of the Total Environment* **734**, 139499. doi:10.1016/J.SCITOTENV.2020.139499